Nonlinear Model Predictive Control for Spacecraft Attitude Tracking with Kalman Filter

Dong-Ting Li, Ai-Guo Wu*, Peng Li
School of Mechanical Engineering and Automation
Harbin Institute of Technology (Shenzhen)
Shenzhen, China
ag.wu@163.com

2020 Chinese Automation Congress (CAC) | 978-1-7281-7687-1/20/$31.00 ©2020 IEEE | DOI: 10.1109/CAC51589.2020.9326718

***Abstract*—This technical paper provides an attitude tracking strategy by employing a nonlinear model predictive controller (NMPC). To directly use the relative navigation information, the piecewise affine (PWA) model based on the Euler dynamics is adopted. Due to the singularity of Euler angles, a singularity-free strategy is proposed to complete continuous attitude tracking. Consider the sensor uncertainty and disturbance, the Kalman filter is combined with the NMPC framework. Finally, the numerical results are presented to show the control performance.**

***Index Terms*—NMPC, Attitude tracking, singularity-free**

I. Introduction

Spacecraft attitude tracking is widely applied in space missions, e.g., the attitude of the chaser should keep consistent with the target's in autonomous rendezvous and docking (AR&D); the member spacecrafts should track the rotation of leader in spacecraft formation missions.

In recent years, many control strategies are applied in spacecraft attitude tracking. Originating from the optimal control, model predictive control (MPC) [1] [2] has been widely used for the advantage of dealing with constraints both on the states and the control inputs. For a linear system, the ahead predictive states and the corresponding desired states are taken into a predefined optimazation index at each sampling instant. By converting the optimazation to a convex quadratic programming (QP) problem, a control input sequence is calculated online through a QP solver. According to the idea of receding horizon control, the first signal of the sequence is used to control the system actually.

However, most practical models are nonlinear. One way to deal with nonlinear models in NMPC is to solve a nonlinear optimazation problem instead of QP problem. On one hand, there is no analytical solution to most nonlinear optimazation problem, only numerical solution. On the other hand, for a coupling model with strong nolinearity, the online solution process cannot guarantee the real-time of control performance. Another way to deal with nonlinear models is to adopt the approximate linear model, e.g., linearize the nonlinear model at each sampling instant [3]; using the multi-model to approximate [4]; adopting the neural networks [5] [6]. Consider the linearization needs to calculate the covariance matrix of the states in real time which will increase the computation cost and time-delay, the PWA model is adopted in [7] and [8].

In this technical paper, the attitude dynamics described by the Euler rotation is adopted, considering the Euler angles can be obtained from the output of the vision-based or laser-based navigation system. Since the dynamics is highly nonlinear with coupling, solving a constrained nonlinear optimization problem online can not guarantee the real-time performance, the PWA model based on the Euler dynamics is employed. Besides, there exists singularity of the Euler angles, this paper proposes a singularity-free strategy. Furthermore, consider the sensor uncertainty and disturbance, the Kalman filter is employed to eliminate the effects.

II. Control model

Consider the attitude tracking mission, assuming that the attitude information of the target is known or can be estimated by the relative navigation system. In this technical paper, the relative attitude is defined by the Euler rotation from the target's body coordinate frame to the chaser's body coordinate frame with $3-2-1$ sequence. Then the kinematics is described as follows,

$$\begin{pmatrix} \dot{\phi} \\ \dot{\theta} \\ \dot{\psi} \end{pmatrix} = \frac{1}{c(\theta)} \begin{pmatrix} c(\theta) & s(\phi)s(\theta) & c(\phi)s(\theta) \\ 0 & c(\phi)c(\theta) & -s(\phi)c(\theta) \\ 0 & s(\phi) & c(\phi) \end{pmatrix} \begin{pmatrix} \omega_1 \\ \omega_2 \\ \omega_3 \end{pmatrix}, \tag{1}$$

where $s(\cdot) \triangleq \sin(\cdot)$, $c(\cdot) \triangleq \cos(\cdot)$; $\phi(t),\ \theta(t),\ \psi(t)$ (rad) are the roll, pitch and yaw angles; for $i = (1,\ 2,\ 3)$, ω_i (rad/s) denote the angular velocities.

The Euler dynamics is given as

$$\begin{cases} J_1\dot{w}_1 = (J_2 - J_3)\omega_2\omega_3 + M_1, \\ J_2\dot{w}_2 = (J_3 - J_1)\omega_1\omega_3 + M_2, \\ J_3\dot{w}_3 = (J_1 - J_2)\omega_1\omega_2 + M_3, \end{cases} \tag{2}$$

where J_i is the principal moment of inertia, M_i denotes the input moment, for $i = (1,\ 2,\ 3)$. In this technical paper, the reaction wheels are adopted as the attitude actuators, then the input moments is described by

$$\begin{cases} M_1 = -\tilde{J}_1(\dot{\omega}_1 + \ddot{\alpha}_1 + \dot{\alpha}_3\omega_2 - \dot{\alpha}_2\omega_3) \backsimeq -\tilde{J}_1(\dot{\omega}_1 + \ddot{\alpha}_1), \\ M_2 = -\tilde{J}_2(\dot{\omega}_2 + \ddot{\alpha}_2 + \dot{\alpha}_1\omega_3 - \dot{\alpha}_3\omega_1) \backsimeq -\tilde{J}_2(\dot{\omega}_2 + \ddot{\alpha}_2), \\ M_3 = -\tilde{J}_3(\dot{\omega}_3 + \ddot{\alpha}_3 + \dot{\alpha}_2\omega_1 - \dot{\alpha}_1\omega_2) \backsimeq -\tilde{J}_3(\dot{\omega}_3 + \ddot{\alpha}_3), \end{cases} \tag{3}$$

where $\tilde{J}_i$ is the moments of inertia of the reaction wheel, $\dot{\alpha}_i$ (rad/s) is the speed of wheel, for $i = (1,\ 2,\ 3)$. Linearize

the relation between the spacecraft's angular velocities and the wheels' acceleration, yields

$$\dot{\omega}_i = -\frac{\tilde{J}_i}{J_i}\ddot{\alpha}_i,\ i = 1, 2, 3. \tag{4}$$

By defining the state vector $\boldsymbol{x} = [\phi,\ \theta,\ \psi,\ \omega_1,\ \omega_2,\ \omega_3]^{\mathrm{T}}$, (1)-(4) can be transformed as follows,

$$\dot{\boldsymbol{x}}(t) = A(\boldsymbol{x})\boldsymbol{x}(t) + B\boldsymbol{u}(t), \tag{5}$$

where

$$\boldsymbol{u} = [u_\phi,\ u_\theta,\ u_\psi]^{\mathrm{T}} \tag{6}$$

is the control input, $A(\boldsymbol{x})$ is a state-dependent matrix with

$$A(\boldsymbol{x}) = \begin{pmatrix} 0 & 0 & 0 & 1 & \frac{s(x_1)s(x_2)}{c(x_2)} & \frac{c(x_1)s(x_2)}{c(x_2)} \\ 0 & 0 & 0 & 0 & c(x_1) & -s(x_1) \\ 0 & 0 & 0 & 0 & \frac{s(x_1)}{c(x_2)} & \frac{c(x_1)}{c(x_2)} \\ 0 & 0 & 0 & 0 & \frac{x_6(J_2-J_3)}{J_1} & 0 \\ 0 & 0 & 0 & 0 & 0 & \frac{x_4(J_3-J_1)}{J_2} \\ 0 & 0 & 0 & \frac{x_5(J_1-J_2)}{J_3} & 0 & 0 \end{pmatrix},$$

and

$$B = \begin{pmatrix} 0 & 0 & 0 \\ 0 & 0 & 0 \\ 0 & 0 & 0 \\ \frac{(\tilde{J}_1^2 - J_1\tilde{J}_1)}{{J_1}^2} & 0 & 0 \\ 0 & \frac{(\tilde{J}_2^2 - J_2\tilde{J}_2)}{{J_2}^2} & 0 \\ 0 & 0 & \frac{(\tilde{J}_3^2 - J_3\tilde{J}_3)}{{J_3}^2} \end{pmatrix}.$$

III. NMPC CONTROLLER DESIGN

In this section, the piecewise affine (PWA) model based on the Euler dynamics is used to design the NMPC. Besides, the control input generated by the reaction wheels is assumed limited.

A. Prediction

Based on the time-varying (5), discrete it at each sampling instant, with the state matrix is set as constant during each sampling interval, the set of discrete models make up the PWA model. Denote the state as $\boldsymbol{x}(k)$ at t_k, the prediction horizon as N_p, then the augmented vector of N_p ahead predictive states is

$$\boldsymbol{x}^*(k) = [\boldsymbol{x}^{\mathrm{T}}(k+1|k),\ \boldsymbol{x}^{\mathrm{T}}(k+2|k),\ \ldots,\ \boldsymbol{x}^{\mathrm{T}}(k+N_p|k)]^{\mathrm{T}}, \tag{7}$$

where

$$\begin{cases} \boldsymbol{x}(k+1|k) = A_k\boldsymbol{x}(k) + B_k\boldsymbol{u}(k), \\ \boldsymbol{x}(k+2|k) = A_{k+1}\boldsymbol{x}(k+1) + B_{k+1}\boldsymbol{u}(k+1), \\ \boldsymbol{x}(k+3|k) = A_{k+2}\boldsymbol{x}(k+2) + B_{k+2}\boldsymbol{u}(k+2), \\ \qquad\qquad \vdots \\ \boldsymbol{x}(k+N_p|k) = A_{k+N_p-1}\boldsymbol{x}(k+N_p-1) \\ +B_{k+N_p-1}\boldsymbol{u}(k+N_p-1). \end{cases} \tag{8}$$

Rewritting the above relation as follows,

$$\boldsymbol{x}^*(k) = A_k^*\boldsymbol{x}(k) + \bar{B}_k^*\bar{\boldsymbol{u}}^*, \tag{9}$$

where $A_k^* \in \mathbb{R}^{6N_p\times 6}$ and $\bar{B}_k^* \in \mathbb{R}^{6N_p\times 3N_p}$,

$$A_k^* = \begin{pmatrix} A_k \\ A_{k+1}A_k \\ \vdots \\ \prod_{i=0}^{N_p-1} A_{k+i} \end{pmatrix},$$

$$\bar{B}_k^* = \begin{pmatrix} B_k & \cdots & 0 \\ A_{k+1}B_k & \ddots & \vdots \\ \vdots & \ddots & \vdots \\ \prod_{i=1}^{N_p-1} A_{k+i}B_k & \cdots & B_{k+N_p-1} \end{pmatrix},$$

and

$$\bar{\boldsymbol{u}}^*(k) = [\boldsymbol{u}(k)^{\mathrm{T}},\ \boldsymbol{u}(k+1)^{\mathrm{T}} \ldots\ \boldsymbol{u}(k+N_p-1)^{\mathrm{T}}] \in \mathbb{R}^{3N_p}.$$

In existing papers, the control horizon is always lower than the predictive horizon. Besides, it will be smoother of the system's response to control the increment of the input signal rather than the total input signal. Denote the control horizon as N_c, and the recurive equation of N_c control inputs $\boldsymbol{u}^* \in \mathbb{R}^{3N_c}$ is defined as follows,

$$\begin{cases} \boldsymbol{u}(k) = \Delta\boldsymbol{u}(k) + \boldsymbol{u}(k-1), \\ \boldsymbol{u}(k+1) = \Delta\boldsymbol{u}(k+1) + \Delta\boldsymbol{u}(k) + \boldsymbol{u}(k-1), \\ \qquad\qquad \vdots \\ \boldsymbol{u}(k+N_c-1) = \Delta\boldsymbol{u}(k+N_c-1) + \ldots + \Delta\boldsymbol{u}(k) + \boldsymbol{u}(k-1). \end{cases} \tag{10}$$

Converting (10) to the following compact form,

$$\boldsymbol{u}^*(k) = \Lambda\boldsymbol{u}(k-1) + \Gamma\Delta\tilde{\boldsymbol{u}}(k), \tag{11}$$

where $\Delta\tilde{\boldsymbol{u}}(k) = \sum_{i=0}^{N_c-1} \Delta\boldsymbol{u}(k+i)|i\rangle \in \mathbb{R}^{3N_c}$, $\Lambda = \sum_{i=1}^{N_c} I_3|i\rangle \in \mathbb{R}^{3N_c\times 3}$, and $\Gamma \in \mathbb{R}^{3N_c\times 3N_c}$ is defined as

$$\Gamma = \begin{pmatrix} I_3 & & & \\ I_3 & \ddots & & \\ \vdots & \ddots & \ddots & \\ I_3 & \cdots & \cdots & I_3 \end{pmatrix}$$

By combining with (11), the predictive states is described by

$$\boldsymbol{x}^*(k) = A_k^*\boldsymbol{x}(k) + B_k^*\Lambda\boldsymbol{u}(k-1) + B_k^*\Gamma\Delta\tilde{\boldsymbol{u}}, \tag{12}$$

where $B_k^* \in \mathbb{R}^{6N_p\times 3N_c}$ is the first $3N_c$ columns of $\bar{B}_k^*$,

$$B_k^* = \begin{pmatrix} B_k & \cdots & 0 \\ A_{k+1}B_k & \cdots & 0 \\ \vdots & \ddots & \vdots \\ \prod_{i=1}^{N_p-1} A_{k+i}B_k & \cdots & \prod_{i=N_c}^{N_p-1} A_{k+i}B_{k+N_c-1} \end{pmatrix}. \tag{13}$$

B. Optimazition index

Consider the following optimazation index,

$$\min J(k) = \sum_{i=1}^{N_p} \|\boldsymbol{x}(k+i) - \boldsymbol{x}_d(k+i)\|_Q^2 + \sum_{i=0}^{N_c-1} \|\Delta \boldsymbol{u}(k+i)\|_P^2 \tag{14}$$

where $\boldsymbol{x}_d$ denotes the desired state, P and Q are the positive-definite and semi-positive definite weight matrices. Converting the above optimation index to the following form,

$$\min J(k) = [\boldsymbol{x}_{\mathrm{d}}^*(k) - \boldsymbol{x}^*(k)]^T \tilde{Q} [\boldsymbol{x}_{\mathrm{d}}^*(k) - \boldsymbol{x}^*(k)] + \Delta \tilde{\boldsymbol{u}}^T \tilde{P} \Delta \tilde{\boldsymbol{u}}, \tag{15}$$

where $\boldsymbol{x}_{\mathrm{d}}^*(k) = \sum_{i=1}^{N_p} \boldsymbol{x}_{\mathrm{d}}(k+i)|i\rangle$ denotes the augmented desired states, $\tilde{Q} = \oplus_{i=1}^{N_p} Q$ and $\tilde{P} = \oplus_{i=1}^{N_p} P$.

Define

$$E = \boldsymbol{x}_{\mathrm{d}}^*(k) - A_k^* \boldsymbol{x}(k) - B_k^* \Lambda \boldsymbol{u}(k-1), \tag{16}$$

and substitute (16) into (15), yields

$$\begin{aligned} \min J(k) &= [B_k^* \Gamma \Delta \tilde{\boldsymbol{u}} - E]^T \tilde{Q} [B_k^* \Gamma \Delta \tilde{\boldsymbol{u}} - E] + \Delta \tilde{\boldsymbol{u}}^T \tilde{P} \Delta \tilde{\boldsymbol{u}} \\ &= \frac{1}{2} \Delta \tilde{\boldsymbol{u}}^T H \Delta \tilde{\boldsymbol{u}} + \boldsymbol{f}^T \Delta \tilde{\boldsymbol{u}}^T + E^T \tilde{Q} E, \end{aligned} \tag{17}$$

where $H = 2[\Gamma^T {B_k^*}^{\mathrm{T}} \tilde{Q} B_k^* \Gamma + \tilde{P}]$ and $\boldsymbol{f} = -2\Gamma^{\mathrm{T}} {B_k^*}^{\mathrm{T}} \tilde{Q} E$.

C. Constraints

In practical space mission, the control input is always limited. The constraint of the reaction wheels is described as

$$-\tilde{\boldsymbol{u}}^{\max} \leqslant \Lambda \boldsymbol{u}(k-1) + \Gamma \Delta \tilde{\boldsymbol{u}} \leqslant \tilde{\boldsymbol{u}}^{\max}, \tag{18}$$

where $\tilde{\boldsymbol{u}}^{\max} = \sum_{i=1}^{N_c} \boldsymbol{u}^{\max}|i\rangle \in \mathbb{R}^{3N_c}$ is the augmented vector of $\boldsymbol{u}^{\max} = [u^{\max},\ u^{\max},\ u^{\max}]^{\mathrm{T}}$, $u^{\max}$ is the maximum control input.

Rewritting the above relation as

$$G \Delta \tilde{\boldsymbol{u}} \leqslant \boldsymbol{g} \tag{19}$$

where

$$G = \begin{pmatrix} \Gamma \\ -\Gamma \end{pmatrix},\ \boldsymbol{g} = \begin{pmatrix} \tilde{\boldsymbol{u}}^{\max} - \Lambda \boldsymbol{u}(k-1) \\ \tilde{\boldsymbol{u}}^{\max} + \Lambda \boldsymbol{u}(k-1) \end{pmatrix}.$$

D. Implementation of Kalman filter

Therfore, (17) and (19) constitute a standard QP probelm, which is described by

$$\Delta \tilde{\boldsymbol{u}} = \arg_{\Delta \boldsymbol{u}} J(k), \tag{20}$$

s.t.

$$\begin{cases} \boldsymbol{x}(k|k) = \boldsymbol{x}(k), \\ \boldsymbol{x}^*(k) = A_k^* \boldsymbol{x}(k) + B_k^* \Lambda \boldsymbol{u}(k-1) + B_k^* \Gamma \Delta \tilde{\boldsymbol{u}}, \\ G \Delta \tilde{\boldsymbol{u}} \leqslant \boldsymbol{g}, \end{cases} \tag{21}$$

Then the optimal control input in the optimization problem can be solved by a QP solver. According to the idea of receding horizon control, the first input signal of $\Delta \tilde{\boldsymbol{u}}$ is adopted to control the system actually by adding $\boldsymbol{u}(k-1)$. However, since there exist disturbance and sensor uncertainty, the actual state is described as

$$\begin{cases} \boldsymbol{x}(k+1) = A_k \boldsymbol{x}(k) + B_k(\Delta \boldsymbol{u}(k) + \boldsymbol{u}(k-1)) + w(k), \\ \boldsymbol{z}(k+1) = \boldsymbol{x}(k+1) + v(k), \end{cases} \tag{22}$$

where $\boldsymbol{z}(k+1)$ denotes the observation of $\boldsymbol{x}(k+1)$, $w(k) \sim N(0, Q_w)$ denotes the disturbance, $v(k) \sim N(0, Q_v)$ denotes the sensor uncertainty which can be described by Gaussian white noise. In this paper, the Kalman filter is employed to eliminate the effects, yields

$$\hat{\boldsymbol{x}}(k+1) = \hat{\boldsymbol{x}}^-(k+1) + K_{k+1}(\boldsymbol{z}(k+1) - \hat{\boldsymbol{x}}^-(k+1)), \tag{23}$$

where

$$K_{k+1} = \frac{P_{k+1}^-}{P_{k+1}^- + Q_v}, \tag{24}$$

is the Kalman gain, with

$$P_{k+1}^- = A_k P_k A_k^{\mathrm{T}} + Q_w, \tag{25}$$

$$P_k = (I - K_k) P_k^-, \tag{26}$$

and

$$\hat{\boldsymbol{x}}^-(k+1) = A_k \boldsymbol{x}(k) + B_k(\Delta \boldsymbol{u}(k) + \boldsymbol{u}(k-1)). \tag{27}$$

IV. Singularity-free strategy

In order to avoid the gimbal lock phenomenon, the pitch angle is set within $[-\pi/2,\ \pi/2]$, the roll and yaw angle is set within $[-\pi,\ \pi]$. Take the roll angle as instance, $\phi = -\pi$ and $\phi = \pi$ are the same position but differ by 2π. As shown in Figure 1, consider continous tracking of roll, it will occour that the desired state ϕ_{d} jumps once it reaches π or $-\pi$. However, it is impossible for the actual state ϕ to track the desired state in a short time, especially for an input-constraint system. Therefore, a singularity-free strategy is proposed in this subsection.

The basic idea of the singularity-free strategy is to automatically reset the state once the state reaches the singular point, by designing the reset mechanism. Assuming the rotation of the target spacecraft is continous, then the strategy can choose the correct value from different singular values and reset the state, by the continuity of rotation.

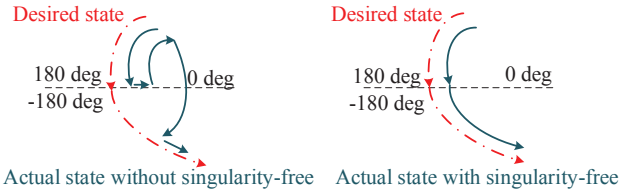

Fig. 1. Singularity

Consider the following two cases, one is ϕ_{d} reaches π $(-\pi)$ but the ϕ doesn't, then we reset the mathematical expression of ϕ_{d} temporarily (doesn't change the physical position) to ensure ϕ moves in the original direction until ϕ reaches the

singularity. The other case is ϕ reaches π $(-\pi)$ but ϕ_{d} doesn't, then we reset ϕ firstly, and change the mathematical expression of ϕ_{d} temporarily to ensure the actual state moves in the original direction until ϕ_{d} reaches the singularity. The detailed strategy of singularity free in presented in Algorithm 2.

Algorithm 1 Singularity free strategy

Require: x_{d} will not repeatedly switch at the singular point
Ensure: $x \in [-n_x\pi, n_x\pi]$ with $n_x = \frac{1}{2}$ or 1

if $\{x_{\mathrm{d}}$ is increasing$\}$ **then**
  if $\{\ x_{\mathrm{d}}(k) = n_x\pi$ && $x(k) < n_x\pi\ \}$ **then**
    $i = 1$
    repeat
      $x_{\mathrm{d}}(k+i) \Leftarrow x_{\mathrm{d}}(k+i) + 2n_x\pi$
      $i \Leftarrow i+1$
    until $x(k+N) = n_x\pi$
    $x(k+N+1) \Leftarrow -n_x\pi$
  else $\{\ x_{\mathrm{d}}(k) < n_x\pi$ && $x(k) = n_x\pi\ \}$
    $x(k+1) = -n_x\pi$
    $i = 1$
    repeat
      $x_{\mathrm{d}}(k+i) \Leftarrow x_{\mathrm{d}}(k+i) - 2n_x\pi$
      $i \Leftarrow i+1$
    until $x_{\mathrm{d}}(k+N) = n_x\pi$
  end if
else $\{x_{\mathrm{d}}$ is decreasing$\}$
  if $\{\ x_{\mathrm{d}}(k) = -n_x\pi$ && $x(k) > n_x\pi\ \}$ **then**
    $i = 1$
    repeat
      $x_{\mathrm{d}}(k+i) \Leftarrow x_{\mathrm{d}}(k+i) - 2n_x\pi$
      $i \Leftarrow i+1$
    until $x(k+N) = -n_x\pi$
    $x(k+N+1) \Leftarrow n_x\pi$
  else $\{\ x_{\mathrm{d}}(k) > -n_x\pi$ && $x(k) = -n_x\pi\ \}$
    $x(k+1) = n_x\pi$
    $i = 1$
    repeat
      $x_{\mathrm{d}}(k+i) \Leftarrow x_{\mathrm{d}}(k+i) + 2n_x\pi$
      $i \Leftarrow i+1$
    until $x_{\mathrm{d}}(k+N) = -n_x\pi$
  end if
end if

Besides, for a discrete system, the state can't always reach the singularity with no error, the solution of the proposed method is considering the actual state reaches the singularity once it reaches a predifined neighbour. There exists inevitable error in this way, our approach is to calculate the error and take it into the next optimazation.

V. Numerical results

In this section, numerical simulations are presented to show the tracking performance. The angular velocity of the target spacecraft is assumed as $[0.02\ ,\ 0.015\ ,\ 0.02\ ]^{\mathrm{T}}\mathrm{rad/s}$. The chaser's inertia matrix in the body frame $\mathcal{F}_{bt}$ is $\mathrm{diag}(50,\ 35,\ 40)\ \mathrm{kg}\cdot\mathrm{m}^2$. The wheels' inertia matrix in the body frame $\mathcal{F}_{bt}$ is $\mathrm{diag}(5,\ 5,\ 5)\ \mathrm{kg}\cdot\mathrm{m}^2$. The maximum control input provided by the reaction wheels is set 1 N. For the parameters in NMPC, the prediction horizon N_p is 30, the control horizon N_c is 15. The simulation duration is set as 500 s and the sampling interval T_s is 0.1 s. The weight matrices P and Q are set $\mathrm{diag}(100,\ 100,\ 100)$ and $\mathrm{diag}(30000,\ 30000,\ 30000,\ 3000,\ 3000,\ 3000)$.

A. Attitude tracking without disturbance and sensor uncertainty

Consider the situation without disturbance and sensor uncertainty. The attitude tracking without singularity-free strategy and with singularity is presented in Figure (2) and Figure (3), it can be seen that the proposed strategy can realize continous tracking with crossing the singularity smoothly. The tracking error is shown in Figure (4), it should be noted that there exist inevitable error during each reset operation, the tracking error can realize lower than 0.5 deg during each reset, and lower than 0.05 deg during the process without reaching the singular points. In addition, the proposed control strategy can satisfy the control input constraint.

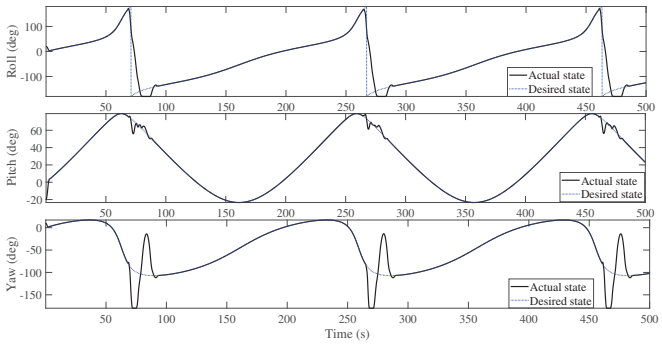

Fig. 2. Attitude tracking without singularity-free

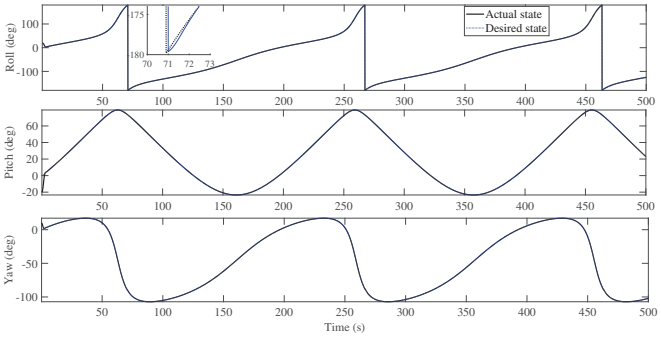

Fig. 3. Attitude tracking with singularity-free

B. Attitude tracking with disturbance and sensor uncertainty

Consider the case with disturbance and sensor uncertainty, assume that $Q_w = \mathrm{diag}(0.25^\circ,\ 0.25^\circ,\ 0.25^\circ,\ 0,\ 0,\ 0)$, and $Q_w = \mathrm{diag}(0.01^\circ,\ 0.01^\circ,\ 0.01^\circ,\ 0,\ 0,\ 0)$, the tracking error without Kalman filter is presented in Figure (5) and the tracking performance with Kalman filter is shown in Figure

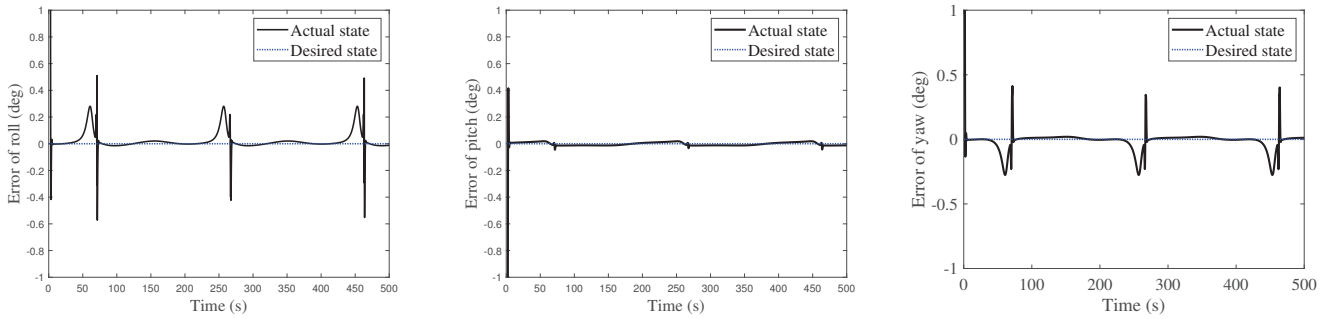

(a) Roll (b) Pitch (c) Yaw

Fig. 4. The tracking error without considering sensor uncertainty

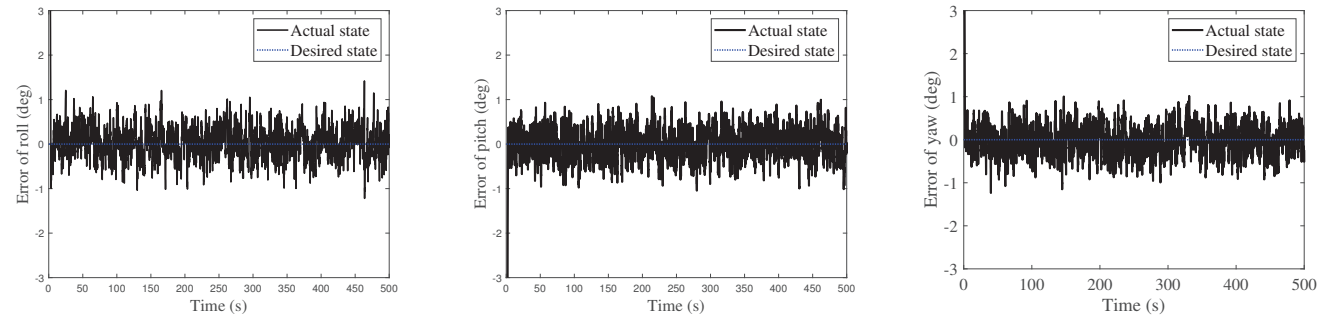

(a) Roll (b) Pitch (c) Yaw

Fig. 5. The tracking error without Kalman filter

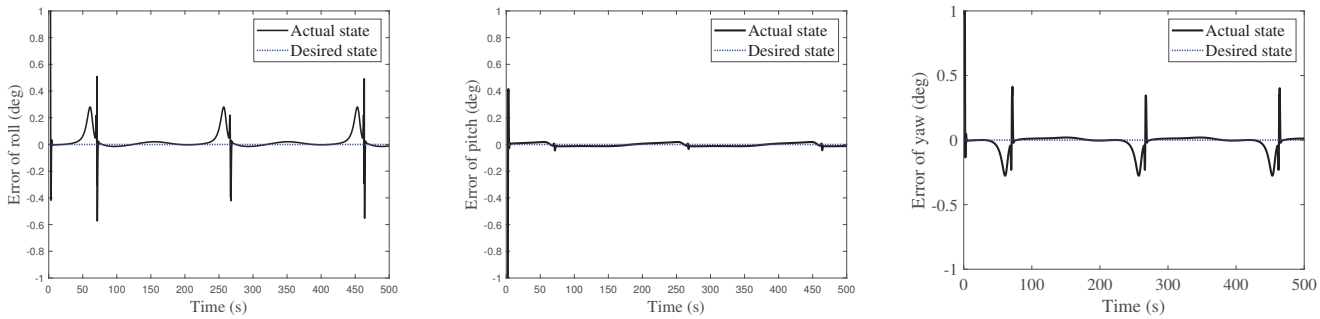

(a) Roll (b) Pitch (c) Yaw

Fig. 6. The tracking error with Kalman filter

(6). It can be seen that the Kalman filter can eliminate the effects of disturbance and sensor uncertainty.

VI. Conclusion

This paper proposes an attitude tracking strategy with NMPC, by using the Euler-based PWA model. Besides, a singularity-free strategy is proposed. It can be witnessed from the simulation results that: (1) the proposed strategy can realize continous attitude tracking; (2) the proposed singularity-free strategy can realize cross the singular points smoothly; (3) disturbance and sensor uncertainty can be elimitaed by employing the Kalman filter.

Future work based on this paper may include: (1) improvement of the robustness of the controller framework; (2) apply the proposed strategy in the 6-DOF pose (position and attitude) tracking.

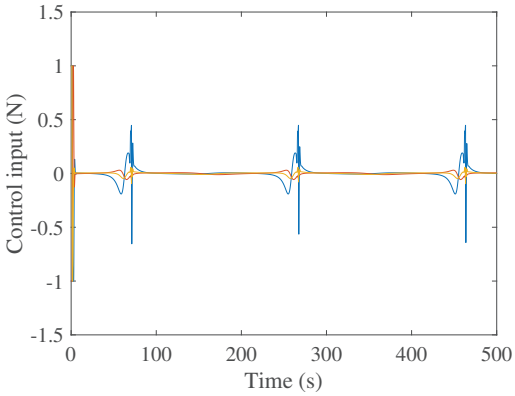

Fig. 7. Control input

REFERENCES

[1] Mayne and Q. David. Model predictive control: Recent developments and future promise. *Automatica*, 50(12):2967–2986, 2014.

[2] D Q Mayne, James B Rawlings, Christopher V Rao, and P O M Scokaert. Survey constrained model predictive control: Stability and optimality. *Automatica*, 36(6):789–814, 2000.

[3] N.L. Ricker and J.H. Lee. Nonlinear model predictive control of the tennessee eastman challenge process. *Computers & Chemical Engineering*, 19(9):961–981, sep 1995.

[4] Jing Zeng, Ding Yu Xue, and De Cheng Yuan. Multi-model predictive control of nonlinear systems. *Journal of Northeastern University*, 30(1):26–29, 2009.

[5] Vincent A. Akpan and George D. Hassapis. Nonlinear model identification and adaptive model predictive control using neural networks. *Isa Transactions*, 50(2):177–194, 2011.

[6] S Piche and B Sayyar-Rodsari. Nonlinear model predictive control using neural networks. *IEEE Control Systems*, 20(3):53–62, 2000.

[7] Unsik Lee and Mehran Mesbahi. Constrained autonomous precision landing via dual quaternions and model predictive control. *Journal of Guidance Control and Dynamics*, 40(2):292–308, 2017.

[8] Peng Li and Zheng H Zhu. Line-of-sight nonlinear model predictive control for autonomous rendezvous in elliptical orbit. *Aerospace Science and Technology*, 69:236–243, 2017.

[9] Peng Li and Zheng H Zhu. Model predictive control for spacecraft rendezvous in elliptical orbit. *Acta Astronautica*, 146:339–348, 2018.

[10] Avishai Weiss, Morgan Baldwin, R S Erwin, and Ilya Kolmanovsky. Model predictive control for spacecraft rendezvous and docking: Strategies for handling constraints and case studies. *IEEE Transactions on Control Systems and Technology*, 23(4):1638–1647, 2015.